

Article

Microstructure and Mechanical Properties of the Ni/Ti/Nb Multilayer Composite Manufactured by Accumulative Pack-Roll Bonding

Nan Ye ¹ , Xueping Ren ^{1,*} and Juhua Liang ²

¹ School of Materials Science and Engineering, University of Science and Technology Beijing, Beijing 100083, China; baggio90@126.com

² Key Laboratory of Materials Physics, Institute of Solid State Physics, Chinese Academy of Sciences, Hefei 230031, China; Liangjuhua0721@126.com

* Correspondence: rxp33@ustb.edu.cn; Tel.: +86-010-8237-6475

Received: 2 February 2020; Accepted: 6 March 2020; Published: 8 March 2020



Abstract: In this work, accumulative pack-roll bonding successfully manufactured the Ni/Ti/Nb multilayer composite. The microstructure evolution and mechanical properties of the composite during the accumulative roll bonding (ARB) process were investigated by scanning electron microscopy (SEM), energy dispersive spectrometer (EDS), transmission electron microscopy (TEM), micro-hardness test, and tensile tests. The results showed that the deformation of each layer was relatively uniform in the initial stage of the ARB process. After the fourth pass, the Ni/Ti interface was still relatively straight, while the Ti/Nb interface was unevenly deformed. After the fourth pass, the microstructure of the Ni layer was equiaxed grains with a decreased grain size of 200 nm, and finer equiaxed grains were observed at the interface. No dynamic recrystallization occurred in the Ti and Nb layers. The laminar structure of the Nb layer was observed, and the grains were oriented parallel to the rolling direction. Moreover, the tensile strength and micro-hardness significantly increased as the number of ARB increased. After five passes of the ARB process, the tensile strength of the composite reached 792.3 MPa, and the micro-hardness of Ni, Ti, and Nb were increased to 270.2, 307.4, and 243.4 HV, respectively.

Keywords: Ni/Ti/Nb multilayer composite; accumulative roll bonding; microstructure; mechanical properties

1. Introduction

Metal multilayer composites generally consist of two or more different metals, which combine the physical properties, chemical properties, and mechanical properties of different metals in order to improve the overall performance of composites [1,2]. Metal multilayer composites have been produced by some bonding technologies: diffusion bonding [3], reaction bonding [4], explosive bonding [5], et al. When compared with several other methods, the roll bonding technology has superiorities, such as simple processes, low cost, and composites can be produced efficiently in large quantities. It has become the major approach for preparing metal composite materials.

Accumulative roll bonding (ARB) is a kind of severe plastic deformation (SPD) technology, which was first proposed by Saito in 1998 and used for preparing ultrafine grain sheets [6]. Compared with other severe plastic deformation techniques, such as high pressure torsion (HPT), equal channel angular pressing (ECAP), repetitive corrugation and straightening (RCS), and cyclic extrusion compression (CEC), ARB technology can produce not only ultra-fine grain sheets with excellent comprehensive properties, but also metal multilayer composites [7–11]. In recent years, many scholars have successfully

prepared multilayer metal composites by the ARB process, such as Al/Mg [12–14], Al/Ti [15,16], Al/Cu [17], and Al/Ni [18,19], etc. Some scholars have also investigated the tri-metal composites, such as Al/Cu/Sn [20], Al/Cu/Mn [21], Al/Cu/Ni [22], Al/Zn/Cu [23], and Al/Ti/Mg [24], etc. For the tri-metal composite, Al with low hardness and good deformability is generally used as the matrix, which is beneficial to the interface bonding in the ARB process. However, there is insufficient research on composites that are composed of three metals with high strength and hardness. Cold-roll bonding must have a large reduction to achieve interface bonding, which is difficult for the metal with high hardness. Therefore, the sample must be heated for roll-bonding, where oxidation on the metal surface might occur. However, these problems can be well solved by a pack-roll bonding process with an internal vacuum.

The pack-roll bonding mainly stacks the metal sheets into a pack and performs vacuum sealing treatment to prevent the oxidation of the metal surfaces during the hot rolling process. It can enhance the interface bonding strength and improves the mechanical properties of composites.

Pure titanium is a hexagonal close-packed structure with low density, high specific strength, and strong corrosion resistance. Pure nickel is a face-centered cubic structure with high conductivity and thermal conductivity, strong toughness, and excellent plastic processing performance. Pure niobium has a high melting point, thus adding niobium can improve the high-temperature performance of the composite.

In this work, commercial pure Ni, Ti, and Nb are used as the raw materials, and accumulative pack-roll bonding manufactures the Ni/Ti/Nb multilayer composite. Scanning electron microscopy (SEM), transmission electron microscopy (TEM), Energy Dispersive Spectrometer (EDS), micro-hardness tests, and tensile tests have been utilized to investigate the microstructure evolution, the interface diffusion, and the mechanical properties.

2. Experimental Procedures

In this work, commercial pure Ni, Ti, and Nb with a thickness of 1 mm were used as raw materials. Table 1 shows the chemical compositions of Ni, Ti, and Nb.

Table 1. Chemical composition of raw materials.

Materials	Element (wt. %)								
	Nb	Ni	Ti	Cu	Si	Fe	Mn	Zn	C
Ni	-	Bal	-	0.002	0.01	0.01	0.03	-	0.011
Ti	-	-	Bal	0.01	0.4	0.3	-	0.04	0.01
Nb	Bal	-	-	-	0.001	0.001	0.03	-	0.003

The raw materials were cut into a dimension of 120 mm × 55 mm × 1 mm. The three kinds of metal sheets were degreased in acetone and polished with a diameter of 0.3 mm wire stainless steel brush. Two Ni, Ti sheets, and one Nb sheet were neatly stacked in the order of “Ni-Ti-Nb-Ti-Ni”. The raw materials were placed into a pack (Figure 1a shows the pack size), which was made of Q235 steel and pre-annealed at 800 °C. The pack was sealed by argon arc welding and vacuumed (as shown in Figure 1b).

The sample was heated in an electric resistance furnace (Beijing US-China New Technology Co., Beijing, China) for 10 min. at 500 °C, and the non-lubricated rolling process was carried out with a total reduction of 66.7% (Von Mises equivalent strain $\epsilon = 1.27$). After the first pass, the bonded sheets were removed from the pack and then cut into three by a shearing machine. Metal sheets were degreased in acetone again, and the surfaces were brushed with a steel brush and stacked. Subsequently, the stacks were placed into a pack with sealed and vacuumed, and the rolling process was continued with a total reduction of 66.7%. The rolling process (as shown in Figure 2) was repeated up to five passes (Von Mises equivalent strain $\epsilon = 6.35$), which were carried out with no lubrication on a two-high mill with a roll diameter of 350 mm. The roll speed was set to 10 rpm during the ARB process.

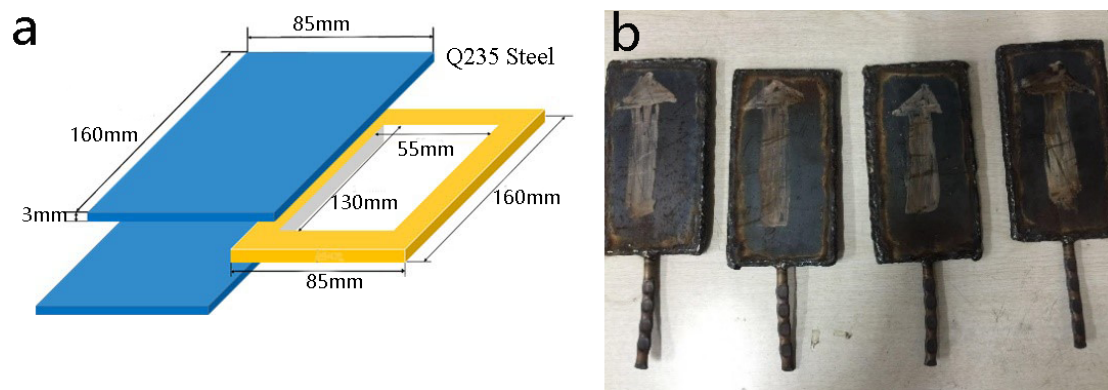


Figure 1. Schematic of the pack: (a) the size of the pack, (b) the packs were sealed and vacuumed.

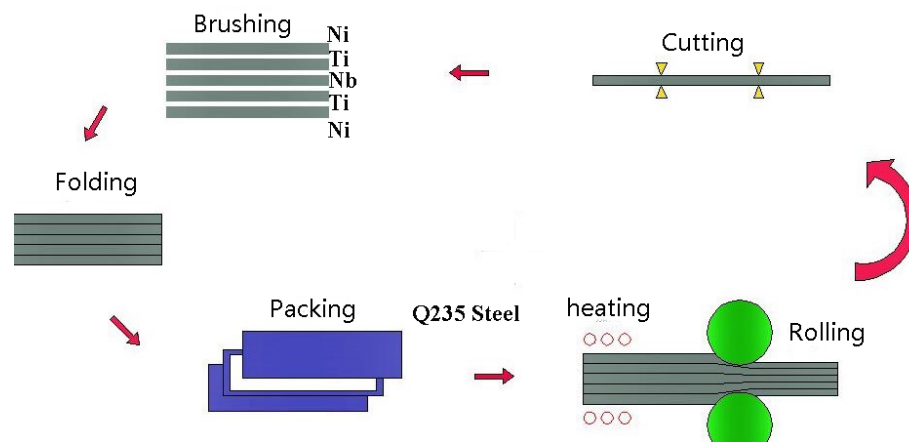


Figure 2. Schematic of the accumulative pack-roll bonding.

Scanning electron microscopy (FEI Quanta 450 FEG, FEI, Hillsboro, OR, USA) and transmission electron microscopy (TEM, Tecnai G2 F20, FEI, Hillsboro, OR, USA) were used to observe the microstructure of the composite. The diffusion data of each element at the interface of the composite material were collected by Energy Dispersive Spectrometer (EDS, FEI, Hillsboro, OR, USA) to characterize the interface diffusion of samples. The Vickers micro-hardness (HV) of each layer of the composite was measured by the micro-hardness tester (HXD-1000TM, Sh-opt Co, Shanghai, China) at a load of 100 g for 15 s. Five points on each metal were measured for hardness and then averaged. The tensile test was carried out using a WDW-200D microcomputer-controlled electronic universal material testing machine (Sh-opt Co, Shanghai, China), with a strain rate of $1 \times 10^{-3} \text{ s}^{-1}$. The tensile sample was processed in the rolling direction. The gauge length and width of the tensile samples were 10 mm and 3 mm.

3. Results and Discussion

3.1. Microstructure Evolution

Figure 3 shows the microstructure of the Ni/Ti/Nb multilayer composite on the RD-ND plane during different ARB passes. The three metals were uniformly distributed, and the thickness of layers was gradually reduced in the normal direction. After three passes of the ARB process, the interfaces of layers were relatively straight, and no obvious necking and fracturing appeared. After the fourth pass, the Ni/Ti interface was still straight for the reason that the mechanical properties of Ni and Ti were similar. However, uneven deformation appeared at the Ti/Nb interface and necking occurred in the Ti layer and Nb layer, as the plastic instabilities occurred due to the differences in mechanical and flow properties of layers at the time of the co-deformation of dissimilar metals [24]. Some shear bands

at an angle of 45° to the rolling direction appeared after the fifth pass of the ARB process. Multiple factors led to the formation of the shear bands. Motevalli et al. [24] reported that shear bands were formed as a result of the slip system that was activated in the softer matrix, and Qu et al. [25] found that such phenomenon was the result of the difference in the flow properties. Moreover, Alizadeh [21] indicated that the formation of the shear bands was due to in-plane shear stress at the interface on the adjacent layers. Similar results were found in other studies on metal composites [17–19,24–28]. These studies indicated that relatively hard metals were prone to local necking and fracturing during the ARB process. As the number of ARB passes increased, hard metals were separated and evenly distributed in soft layers. Uneven deformation occurred locally in layers to cause a change in stress state when the accumulative strain reached a certain level due to the different plastic deformation of dissimilar metals. Generally speaking, the non-uniform interaction between the different layers led to change the heterogeneous structure of the interface, which results in the necking phenomenon and breakdown in the hard layers [20].

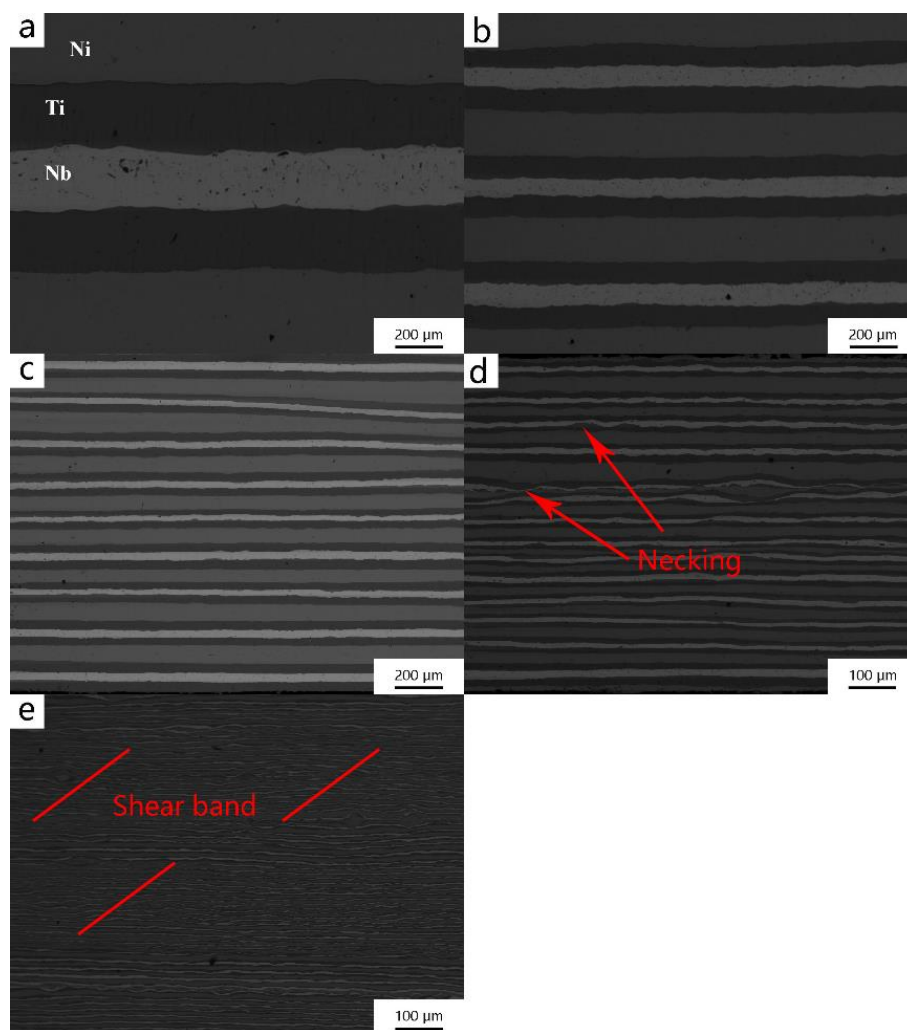


Figure 3. SEM micrographs of the Ni/Ti/Nb composite: (a) after the first pass, (b) after the second pass, (c) after the third pass, (d) after the fourth pass, and (e) after the fifth pass.

Figure 4 is a TEM micrograph of the composite after different ARB passes. Figure 4a,b, respectively, illustrate the microstructure of the Ni layer after the third and fifth passes. The grain size of Ni was significantly reduced as the number of the ARB passes increased, and then fine equiaxed grains with a size of approximately 200 nm appeared after the five passes. Nickel had a face-centered cubic structure, and the dislocation slip caused the dislocation density inside the grain and at the grain

boundary to increase rapidly, and the interaction between the dislocations was plugged and then entangled to form dislocation cells. Subsequently, the dislocation cells evolved into grain boundaries, forming fine grains. The refinement mechanism was that the dislocation interfaces formed, and the grains were continuously divided.

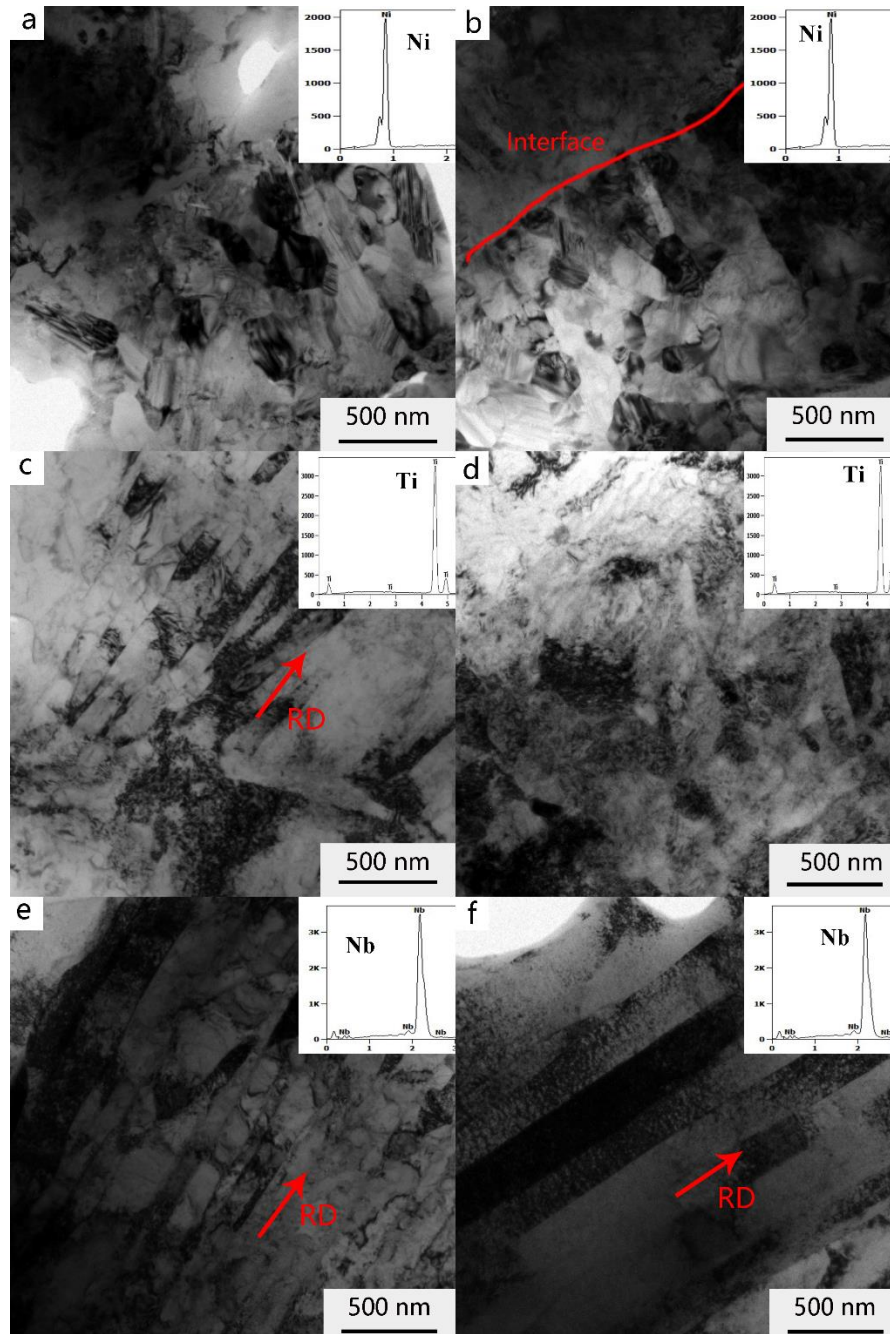


Figure 4. Transmission electron microscopy (TEM) micrographs of the Ni/Ti/Nb composite: (a) Ni layer after third pass, (b) Ni layer after the fifth pass, (c) Ti layer after the third pass, (d) Ti layer after the fifth, (e) Nb layer after the third pass, and (f) Nb layer after the fifth pass.

In addition, some finer equiaxed grains were found near the interface, and the dislocation density was larger than that away from the interface. In the ARB process, severe shear strain was generated near the interface of the sample due to the different flow rates of dissimilar metals, resulting in grain refinement and large dislocation density.

Figure 4c,d, respectively, show the microstructure of the Ti layer after the 3rd and 5th passes. The Ti layer grains were flattened and elongated in the rolling direction, forming a laminar structure after the third pass of the ARB process, and there was a significant density dislocation between the laths. With the increasing number of the ARB passes, a large number of dislocations were still apparent in the microstructure of the Ti layer. It was indicated that no dynamic recovery and recrystallization occurred in the Ti layer.

Figure 4e,f, respectively, illustrate the microstructure of the Nb layer after the 3rd and 5th passes. The laminar structure of the Nb layer was observed, and the grains were oriented parallel to the rolling direction. From the third pass to the fifth pass, the laminar structure was always seen in the Nb layer. This phenomenon was due to the high recrystallization temperature of Nb, and the ARB process at 500 °C was insufficient for providing the energy required for dynamic recrystallization.

3.2. Interface Investigation

ARB is a type of cold-press welding, which is mainly divided into three stages: surface oxide film cracking, metal point bonding, and metal face bonding. The effects of rolling pressure and friction force cause stress concentration and locally asperities fracture. The surface oxide film breaks, and then dissimilar metals contact each other to form point bonding. As the number of rolling passes increases, surface bonding was formed between the layers due to the further plastic deformation.

In general, elemental diffusion occurs at the interface during the ARB process, and the interface bonding mode is similar to that of powder metallurgy (mechanical alloying). Mechanical alloying involves three main mechanisms: (1) atomic displacement due to mechanical force, (2) diffusion around vacancies, and (3) produced vacancies as a result of plastic deformation [18,19,24].

Figure 5 shows the EDS analysis of the interface line after different passes. It could be seen that, the element diffusion distance increased with the increasing number of ARB process. It could be found that the element diffusion distance of the Ni/Ti interface was always close to that of the Nb/Ti interface. In fact, the interface diffusion distance was related to the nature of the elements [24]. The diffusion activation energies of Ni and Nb in the Ti matrix are 137 kJ/mol [29] and 129.9 kJ/mol [30], respectively (found in Springer Materials database). It could be found that the diffusion capacities of the two metals in the Ti matrix were close, so the element diffusion distance at the Ni/Ti interface was not much different from the Nb/Ti interface.

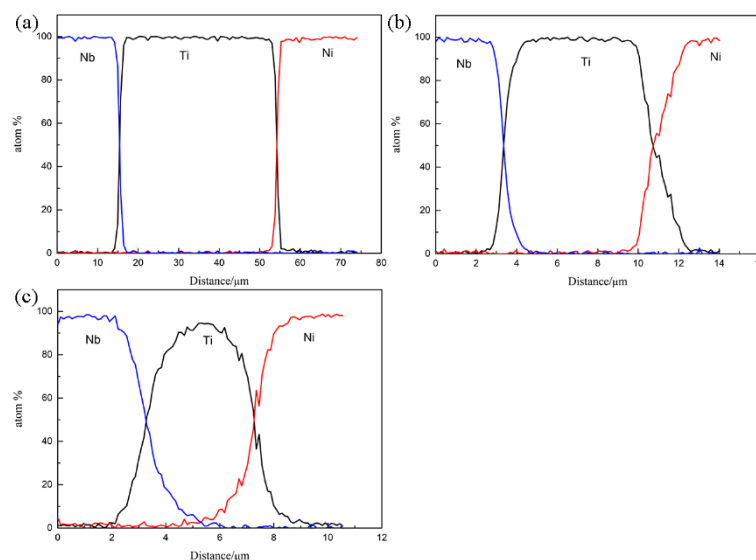


Figure 5. The interface diffusion distance of the Ni/Ti/Nb composite: (a) after the third pass, (b) after the fourth pass, and (c) after the fifth pass.

As the number of ARB pass increased, the element diffusion distance between the interfaces increased, which indicated that the interface bonding strength was enhanced. Metal bonds formed due to the balance of attractive and repulsive forces and the reduction in interface energy. This interface diffusion due to deformation has a positive effect on improving the mechanical properties of the composite.

3.3. Mechanical Properties

3.3.1. Tensile Test

A tensile test was conducted in order to study the effect of ARB cycle on the mechanical properties of composites. Figure 6a shows the stress-strain curves of the composite after different passes. Figure 6b illustrates the change in the mechanical properties of the composite with different ARB passes. The strength of the composite significantly increased and the elongation decreased as compared with the raw materials after the first pass. As the number of ARB passes increased, the strength of the composite gradually increased and the elongation decreased. The tensile strength of the composite reached 792.3 MPa after the fifth pass.

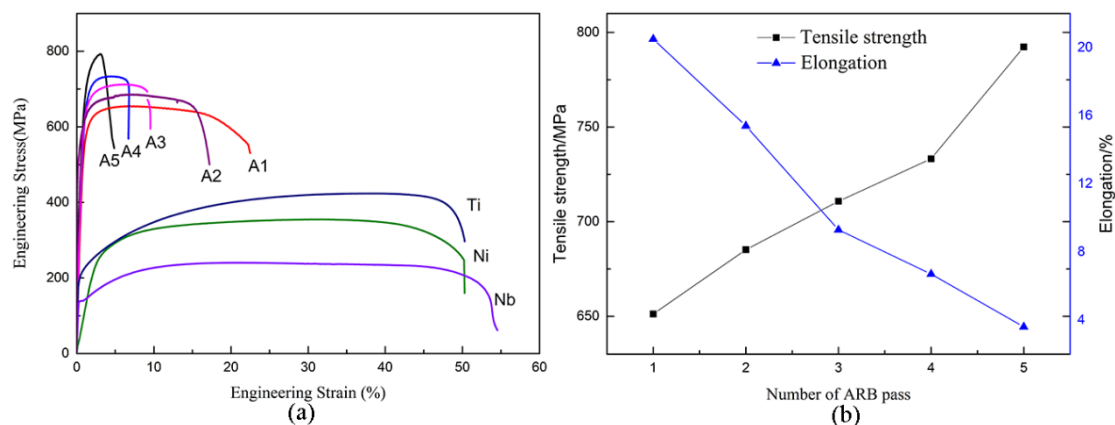


Figure 6. Mechanical properties of the Ni/Ti/Nb multilayer composite: (a) stress-strain curves, (b) variations of tensile strength and elongation versus the number of accumulative roll bonding (ARB) passes.

Generally, there were two main strengthening mechanisms for the improvement of composite strength: work hardening and grain refinement. In the initial stage of ARB, strain hardening or dislocation strengthening played a major role in improving composite strength. With the increasing number of ARB passes, the microstructure of the composite was gradually refined and uniformed, and dynamic recovery and recrystallization occurred. The higher strength of the composite was related to grain refinement (ultrafine grains played a major role in strengthening) [24,31]. In the initial stage of the ARB process, the deformation of each layer was relatively uniform during the ARB process and inter-laminar fractures rarely occurred. A large number of evenly distributed interfaces hindered the slip and expansion of dislocations due to the increased interface. Therefore, the strength of the composites increased. With the increasing number of ARB pass, local uneven deformation and necking occur in the composite material, and hence the elongation is significantly reduced.

3.3.2. Micro-Hardness

Figure 7 illustrates the variation of average micro-hardness with respect to the number of ARB pass. As the number of the ARB pass increased, the average micro-hardness of layers increased gradually due to the work hardening and grain strengthening. After the first pass, the micro-hardness of the three metals increased rapidly, and the rate of increase decreased in the subsequent process. It was reported that [18] the work hardening affected in the initial stage of the ARB process, the effect of

improving the micro-hardness was much higher than the later grain refinement. After five passes, the average micro-hardness of Ni, Ti, and Nb increased from 161.8, 173.4, and 78.2 HV to 270.2, 307.4, and 243.4 HV, which increased by 67.0%, 77.3%, and 211.3%, respectively. In the ARB process, the Nb layer kept a laminar structure throughout the process, and no dynamic recovery and recrystallization occurred, so the hardness growth rate of Nb was the highest. Additionally, the micro-hardness growth rate of Ni was the lowest due to the dynamic recovery and recrystallization of Ni.

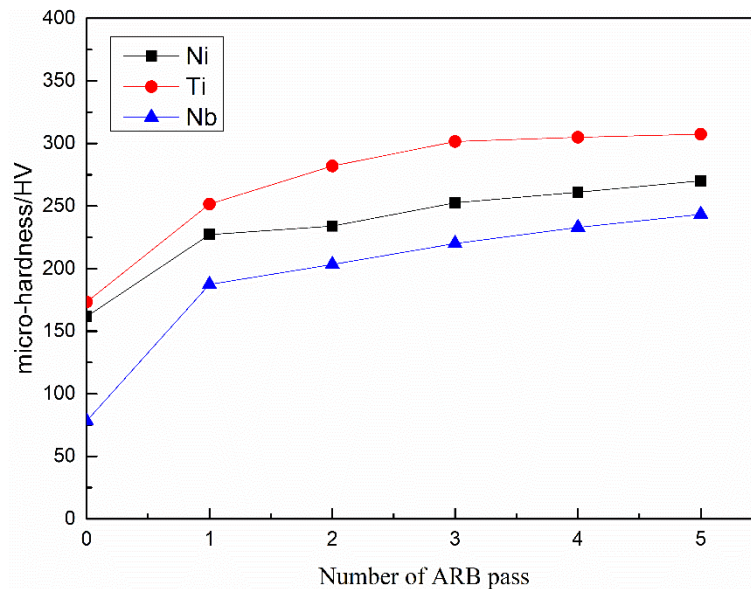


Figure 7. Variations of micro-hardness versus the number of the ARB pass.

3.3.3. Fractography

Figure 8 shows the fracture surface of the composite after tensile tests. Visible interface separation was evident in the fracture surface after the third pass. After the fifth pass, the interface was combined well in most areas and few visible delaminations in the tensile sample. It was indicated that, as the number of the ARB pass increased, the interfacial bonding strength of the composite was gradually enhanced.

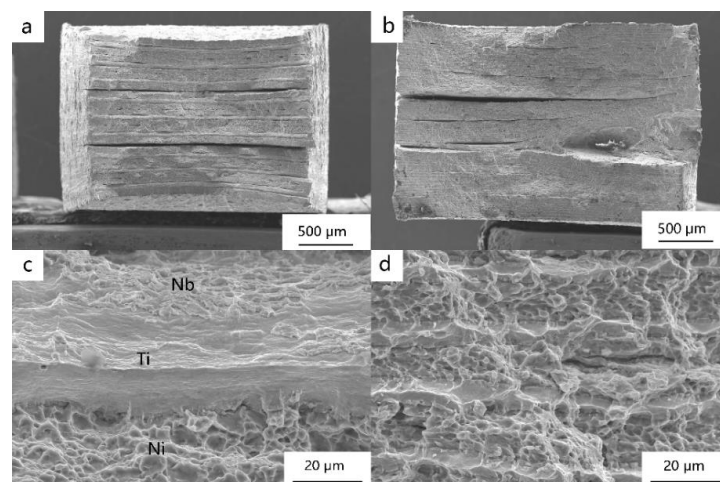


Figure 8. Tensile fracture surfaces of the Ni/Ti/Nb multilayer composite: (a) after the third pass, (b) after the fifth pass, (c) high magnification after the third pass, and (d) high magnification after the fifth pass.

Figure 8c,d show the fracture surface of the composite at higher magnifications. It could be seen that Nb and Ti were nearly integrated after the third pass. There were some shallow dimples on the fracture surface of the Nb layer, which was a ductile fracture, while it exhibited a quasi-cleavage fracture on the surface of the Ti layer. Furthermore, there were apparent dimples on the fracture surface of the Ni layer, which was the dimple fracture. This phenomenon was related to the microstructure of the three metals (as shown in Figure 4). After the fifth pass, the composite became a whole due to the enhanced interface bonding. The dimples on the fracture surface were not as deep as that in the third pass, and the equiaxed dimples became shallow and small shear dimples due to shear stress. Therefore, the fracture surface exhibited a shear fracture.

4. Conclusions

In this study, accumulative pack-roll bonding manufactured the Ni/Ti/Nb multilayer composite. The microstructure evolution, the interface diffusion, and the mechanical properties were investigated. The results can be listed, as follows:

- (1) The Ni/Ti/Nb multilayer composite was manufactured by ARB technology up to five passes. The deformation of each layer was relatively uniform in the initial stage of the ARB process. After the fourth pass, the Ni/Ti interface was still relatively straight, while the Ti/Nb interface was unevenly deformed.
- (2) As the number of ARB process increased, the grain size of the composite decreased. After five passes, the microstructure of Ni was equiaxed grains with a decreased grain size of 200 nm, and finer equiaxed grains were visible near the interface of the Ni layer. No dynamic recrystallization occurred in the Ti and Nb layers. The laminar structure of the Nb layer was observed and the grains were oriented parallel to the rolling direction.
- (3) As the number of ARB process increased, the tensile strength of the composite increased significantly and the elongation decreased. After five passes, the tensile strength of the composite reached 792.3 MPa.
- (4) The micro-hardness of the three metals gradually increased during the ARB process, especially a rapid increase appeared after the first pass. After five passes, the micro-hardness of the Ni, Ti, and Nb were increased to 270.2, 307.4, and 243.4 HV.

Author Contributions: N.Y. and X.R. conceived and designed the experiments; N.Y. performed the experiments; N.Y. and J.L. analyzed the data; X.R. contributed reagents/materials/analysis tools; N.Y. wrote the paper. All authors have read and agreed to the published version of the manuscript.

Funding: This research and the APC were funded by the Young Scientists Fund of the National Natural Science Foundation of China (Grant No. 51505450, 51605457).

Acknowledgments: The authors would like to thank the support from Mr. Shuiping Hu for the help on experimentation.

Conflicts of Interest: The authors declare no conflict of interest.

References

1. Wadsworth, J.; Lesuer, D.R. Ancient and modern laminated composites—From the Great Pyramid of Gizeh to Y2K. *Mater. Charct.* **2000**, *45*, 289–313. [[CrossRef](#)]
2. Li, Y.P.; Zhang, G.P.; Wang, W.; Tan, J.; Zhu, S.J. On interface strengthening ability in metallic multilayers. *Scr. Mater.* **2007**, *57*, 117–120. [[CrossRef](#)]
3. Cao, J.; Song, X.G.; Wu, L.Z.; Qi, J.L.; Feng, J.C. Characterization of Al/Ni multilayers and their application in diffusion bonding of TiAl to TiC cermet. *Thin Solid Film.* **2012**, *520*, 3528–3531. [[CrossRef](#)]
4. Cao, J.; Feng, J.C.; Li, Z.R. Microstructure and fracture properties of reaction-assisted diffusion bonding of TiAl intermetallic with Al/Ni multilayer foils. *J. Alloy. Compd.* **2008**, *466*, 363–367. [[CrossRef](#)]

5. Fan, M.; Yu, W.; Wang, W.; Guo, X.; Jin, K.; Miao, R.; Hou, W.; Kim, N.; Tao, J. Microstructure and mechanical properties of thin-multilayer Ti/Al laminates prepared by one-step explosive bonding. *J. Mater. Eng. Perform.* **2017**, *26*, 277–285. [[CrossRef](#)]
6. Saito, Y.; Tsuji, N.; Utsunomiya, H.; Sakai, T.; Hong, R.G. Ultra-fine grained bulk aluminum produced by accumulative roll-bonding (ARB) process. *Scr. Mater.* **1998**, *39*, 1221–1227. [[CrossRef](#)]
7. Valiev, R.Z.; Islamgaliev, R.K.; Alexandrov, I.V. Bulk nanostructured materials from severe plastic deformation. *Prog. Mater. Sci.* **2000**, *45*, 103–107. [[CrossRef](#)]
8. Segal, V.M. Equal channel angular extrusion: From macromechanics to structure formation. *Mater. Sci. Eng. A* **1999**, *271*, 322–333. [[CrossRef](#)]
9. Sakai, G.; Horita, Z.; Langdon, T.G. Grain refinement and superplasticity in an aluminum alloy processed by high-pressure torsion. *Mater. Sci. Eng. A* **2005**, *393*, 344–351. [[CrossRef](#)]
10. Tsuji, N.; Ito, Y.; Saito, Y.; Minamino, Y. Strength and ductility of ultrafine grained aluminum and iron produced by ARB and annealing. *Scr. Mater.* **2002**, *47*, 893–899. [[CrossRef](#)]
11. Azushima, A.; Kopp, R.; Korhonen, A.; Yang, D.Y.; Micari, F.; Lahoti, G.D.; Groche, P.; Yanagimoto, J.; Tsuji, N.; Rosochowski, A.; et al. Severe plastic deformation (SPD) processes for metals. *CIRP Ann. Manuf. Technol.* **2008**, *57*, 716–735. [[CrossRef](#)]
12. Chang, H.; Zheng, M.Y.; Gan, W.M.; Wu, K.; Maawad, E.; Brokmeier, H.G. Texture evolution of the Mg/Al laminated composite fabricated by the accumulative roll bonding. *Scr. Mater.* **2009**, *61*, 717–720. [[CrossRef](#)]
13. Wu, K.; Chang, H.; Maawad, E.; Gan, W.M.; Brokmeier, H.G.; Zheng, M.Y. Microstructure and mechanical properties of the Mg/Al laminated composite fabricated by accumulative roll bonding (ARB). *Mater. Sci. Eng. A* **2010**, *527*, 3073–3078. [[CrossRef](#)]
14. Chang, H.; Zheng, M.Y.; Xu, C.; Fan, G.D.; Brokmeier, H.G.; Wu, K. Microstructure and mechanical properties of the Mg/Al multilayer fabricated by accumulative roll bonding (ARB) at ambient temperature. *Mater. Sci. Eng. A* **2013**, *543*, 249–256. [[CrossRef](#)]
15. Yang, D.K.; Cizek, P.; Hodgson, P.D.; Wen, C.E. Microstructure evolution and nanograin formation during shear localization in cold-rolled titanium. *Acta Mater.* **2010**, *58*, 4536–4548. [[CrossRef](#)]
16. Yang, D.K.; Cizek, P.; Hodgson, P.D.; Wen, C.E. Ultrafine equiaxed-grain Ti/Al composite produced by accumulative roll bonding. *Scr. Mater.* **2010**, *62*, 321–324. [[CrossRef](#)]
17. Eizadjou, M.; Talachi, A.K.; Manesh, H.D.; Shahabi, H.S.; Janghorban, K. Investigation of structure and mechanical properties of multi-layered Al/Cu composite produced by accumulative roll bonding (ARB) process. *Compos. Sci. Technol.* **2008**, *68*, 2003–2009. [[CrossRef](#)]
18. Mozaffari, A.; Hosseini, M.; Manesh, H.D. Al/Ni metal intermetallic composite produced by accumulative roll bonding and reaction annealing. *J. Alloy. Compd.* **2011**, *509*, 9938–9945. [[CrossRef](#)]
19. Mozaffari, A.; Manesh, H.D.; Janghorban, K. Evaluation of mechanical properties and structure of multilayered Al/Ni composites produced by accumulative roll bonding (ARB) process. *J. Alloy. Compd.* **2010**, *489*, 103–109. [[CrossRef](#)]
20. Mahdavian, M.M.; Khatami-Hamedani, H.; Abedi, H.R. Macrostructure evolution and mechanical properties of accumulative roll bonded Al/Cu/Sn multilayer composite. *J. Alloy. Compd.* **2017**, *703*, 605–613. [[CrossRef](#)]
21. Alizadeh, M.; Samiei, M. Fabrication of nanostructured Al/Cu/Mn metallic multilayer composites by accumulative roll bonding process and investigation of their mechanical properties. *Mater. Des.* **2014**, *56*, 680–684. [[CrossRef](#)]
22. Shabani, A.; Toroghinejad, M.R.; Shafyei, A. Fabrication of Al/Ni/Cu composite by accumulative roll bonding and electroplating processes and investigation of its microstructure and mechanical properties. *Mater. Sci. Eng. A* **2012**, *558*, 386–393. [[CrossRef](#)]
23. Mahdavian, M.M.; Ghalandari, L.; Reihanian, M. Accumulative roll bonding of multilayered Cu/Zn/Al: An evaluation of microstructure and mechanical properties. *Mater. Sci. Eng. A* **2013**, *579*, 99–107. [[CrossRef](#)]
24. Motevalli, P.D.; Eghbali, B. Microstructure and mechanical properties of Tri-metal Al/Ti/Mg laminated composite processed by accumulative roll bonding. *Mater. Sci. Eng. A* **2015**, *628*, 135–142. [[CrossRef](#)]
25. Qu, P.; Zhou, L.; Acoff, V.L. Deformation Textures of Aluminum in a Multilayered Ti/Al/Nb Composite Severely Deformed by Accumulative Roll Bonding. *Mater. Charct.* **2015**, *107*, 367–375. [[CrossRef](#)]
26. Ghalandari, L.; Moshksar, M.M. High-strength and high-conductive Cu/Ag multilayer produced by ARB. *J. Alloy. Compd.* **2010**, *506*, 172–178. [[CrossRef](#)]

27. Dehsorkhi, R.N.; Qods, F.; Tajally, M. Investigation on microstructure and mechanical properties of Al–Zn composite during accumulative roll bonding (ARB) process. *Mater. Sci. Eng. A* **2011**, *530*, 63–72. [[CrossRef](#)]
28. Ghalandari, L.; Mahdavian, M.M.; Reihanian, M. Microstructure evolution and mechanical properties of Cu/Zn multilayer processed by accumulative roll bonding (ARB). *Mater. Sci. Eng. A* **2014**, *593*, 145–153. [[CrossRef](#)]
29. Hood, G.M.; Schultz, R.J. Ultra-fast solute diffusion in α -Ti and α -Zr. *Philos. Mag.* **1972**, *26*, 329–336. [[CrossRef](#)]
30. Gibbs, G.B.; Graham, D.; Tomlin, D.H. Diffusion in titanium and titanium-niobium alloys. *Philos. Mag.* **1963**, *8*, 1269–1282. [[CrossRef](#)]
31. Mashhadi, A.; Atrian, A.; Ghalandari, L. Mechanical and microstructural investigation of Zn/Sn multilayered composites fabricated by accumulative roll bonding (ARB) process. *J. Alloy. Compd.* **2017**, *727*, 1314–1323. [[CrossRef](#)]



© 2020 by the authors. Licensee MDPI, Basel, Switzerland. This article is an open access article distributed under the terms and conditions of the Creative Commons Attribution (CC BY) license (<http://creativecommons.org/licenses/by/4.0/>).